Approximating infinite-***k*** representations: surface relaxations and work functions of Al(001) and Be(0001)

1997 J. Phys.: Condens. Matter 9 8359

(http://iopscience.iop.org/0953-8984/9/40/004)

J. Phys.: Condens. Matter **9** (1997) 8359–8368. Printed in the UK PII: S0953-8984(97)82103-0

Approximating infinite-*k* representations: surface relaxations and work functions of Al(001) and Be(0001)

Daniel Gebreselasie and G A Benesh

Department of Physics, Baylor University, Waco, TX 76798, USA

Received 24 February 1997, in final form 28 July 1997

Abstract. Self-consistent techniques, such as the linearized augmented plane wave (LAPW) and surface embedding Green function (SEGF) methods, frequently yield calculated quantities which show damped oscillatory behaviour as a function of the number of special $\boldsymbol{k}$-points. In the present work, the oscillatory dependence has been fitted to a damped harmonic oscillator in order to approximate the value corresponding to an infinite number of $\boldsymbol{k}$-points in the Brillouin zone. The asymptotic value, amplitude, frequency, and phase are determined as functions of the damping constant by matching the value and derivative of the damped harmonic oscillator at consecutive turning points. It is shown that the asymptotic value of the damped oscillator may fall within the rms error of the asymptotic value of the fitting function. Results are reported for the surface relaxations and work functions of Al(001) and Be(0001).

1. Introduction

Density functional theory relates an interacting system to a non-interacting system of the same charge density subject to a modified potential. The charge density is usually obtained by summing contributions from all occupied states of the system; for an infinite system, an integration over the infinite number of states in the occupied portion of the Brillouin zone is required. The general practice has been to replace the BZ integral by a weighted sum using sets of special $\boldsymbol{k}$-points and weights in such a way as to minimize the approximation error. However, when only a single set of $\boldsymbol{k}$-points is used, there is no simple way of predicting how close the calculated finite-$\boldsymbol{k}$ results are to the (actual) infinite-$\boldsymbol{k}$ asymptotic values.

Surface embedding Green function studies (incorporating LAPW basis functions) of physical quantities such as the work function, force, and surface relaxation show similar damped oscillatory behaviour with the number of special $\boldsymbol{k}$-points. Such arbitrary damped oscillatory functions can be fitted to a harmonic oscillator by means of a general technique outlined in section 2. (A detailed explanation of the method is given in the appendix.) Once the results for the first few sets of special $\boldsymbol{k}$-points have been fitted to damped harmonic oscillators, the infinite-$\boldsymbol{k}$ asymptotic values can be predicted. In section 3, the method is applied to the Al(001) and Be(0001) surfaces, and comparisons with other theoretical and experimental work are presented.

2. Theory

Self-consistent techniques often yield calculated quantities which show damped oscillatory behaviour as a function of the number of special $\boldsymbol{k}$-points. Let $h(x)$ be an arbitrary damped

0953-8984/97/408359+10$19.50

oscillatory function whose asymptotic value is C. To approximate C (corresponding to an infinite number of $\boldsymbol{k}$-points in the Brillouin zone), it is desirable to fit $h(x)$ to a damped harmonic oscillator of the form

$$g(x) = A + B\,\mathrm{e}^{-\alpha x}\cos(\omega x + \beta). \tag{1}$$

The asymptotic value of the fitting function, A, is then the approximate asymptotic value of the calculated quantity. The method described below assumes that the oscillatory, but not necessarily periodic, function $h(x)$ is known on an interval which contains two consecutive turning points, x_j and x_{j+1}. That is

$$x \in X_j = [x_j - \varepsilon_\ell, x_{j+1} + \varepsilon_r] \tag{2}$$

where ε_ℓ and ε_r are small compared to $x_j - x_{j+1}$.

A damped harmonic oscillator has five parameters that can be adjusted freely to fit the function of interest. These are the asymptotic value (A), the amplitude (B), the damping constant (α), the frequency (ω), and the phase shift (β). The asymptotic value, amplitude, frequency, and phase shift are fixed by matching the value and derivative of the function to be fitted at two consecutive turning points.

The fitting procedure leads to the following expression for the asymptotic value of the damped harmonic oscillator:

$$A_j(\alpha_j, \{\lambda_i\}) = h(x_j) - \frac{h(x_j) - h(x_{j+1})}{1 + \mathrm{e}^{-\alpha_j \pi/\omega_j(\{\lambda_i\})}} \tag{3}$$

where $h(x_j)$ and $h(x_{j+1})$ are the values at the two turning points. (For details, see the appendix.) A_j is thus the approximate infinite-$\boldsymbol{k}$ asymptotic value of $h(x)$.

To obtain some sense of how well the asymptotic value of the damped harmonic oscillator approximates the asymptotic value of the oscillatory function $h(x)$, the method proceeds as follows. First, the fact that succeeding turning points are nearer to the asymptotic value limits the range of C. It must lie between the average value of the two turning points and the value at the second point. That is,

$$C \in Y_j = \left[h(x_{j+1}), \frac{h(x_j) + h(x_{j+1})}{2}\right) \qquad \text{when } h(x_j) > h(x_{j+1}) \tag{4}$$

or

$$C \in Y_j = \left(\frac{h(x_j) + h(x_{j+1})}{2}, h(x_{j+1})\right] \qquad \text{when } h(x_j) < h(x_{j+1}). \tag{5}$$

The error interval may be further reduced by fitting $g(x)$ to $h(x)$ over several intervals. It is shown in the appendix that the rms difference per interval decreases as x increases for subsequent intervals. Thus, the rms difference evaluated over the first interval is greater than the rms interval evaluated over the entire range—and C must lie in the intersection of all error intervals (A33). For other details of the method, please see the appendix.

3. Applications

The approximation technique outlined in section 2 and described in the appendix has been applied to the work function and surface relaxation of the Al(001) and Be(0001) surfaces. The surface embedded Green function (SEGF) method [1, 2] has been used to obtain the charge densities of both surfaces. The SEGF method employs LAPW basis functions and the full potential, with no shape approximation, in the surface region. Surface layers are embedded directly onto an infinite bulk substrate by means of an embedding potential derived from the bulk Green function.

3.1. Al(001)

The calculations were performed using Monkhorst and Pack's special $\boldsymbol{k}$-point sets for a square lattice [3]. The variable x is defined in such a way that consecutive sets of special $\boldsymbol{k}$-points are separated by unity. The lower bound of the first interval, X_1, is set to zero. The function $s(x, \{\lambda_i\})$ is defined as in the appendix ((A11) and following).

3.1.1. Work function. Seven values of the work function were obtained using the 6-, 10-, 15-, 21-, 28-, 36- and 45-special-$\boldsymbol{k}$-point sets. The dependence of the work function on x is depicted in figure 1. It is seen that the work function behaves in an oscillatory manner as $h(x)$. The interval X_1 (with j equal to one) is taken as $X_1 = [0, 5]$. The locations of the turning points, x_1 and x_2, are approximated by Lagrange interpolation as 1.01 and 1.32, respectively.

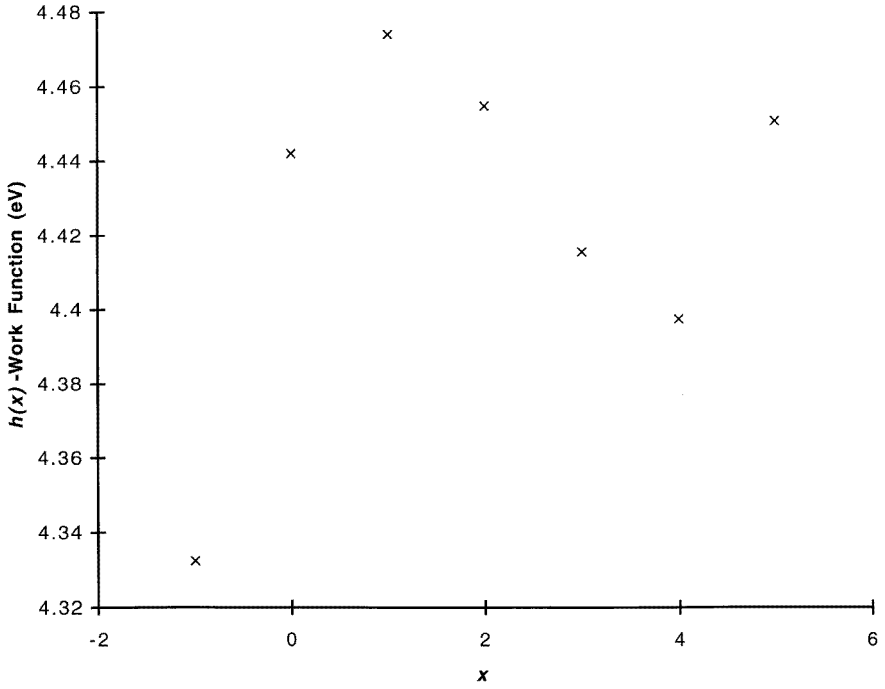

Figure 1. The dependence of the Al(001) work function on x.

The damping constant, $\tilde{\alpha}_1(\lambda)$, that minimizes the rms difference for an arbitrary λ was obtained; the rms differences for the λ were then compared. Figure 2 shows the λ-dependence of the rms difference, $\tilde{r}_1[\tilde{\alpha}_1(\lambda), \lambda]$, and the asymptotic value of the fitting function, $A_1[\tilde{\alpha}(\lambda), \lambda]$. The power of x that leads to a minimum rms difference, $\tilde{\lambda}$, is approximately 0.9. The corresponding rms difference, $\tilde{r}_1[\tilde{\alpha}_1(\tilde{\lambda}), \tilde{\lambda}]$, was calculated to be 0.007 eV. Thus, the Z_1 error interval is given by $Z_1 = [4.428, 4.442]$ eV. The values of the work function at the turning points, $h(x_1)$ and $h(x_2)$, as obtained by Lagrange interpolation are 4.474 and 4.397 eV, respectively. Hence, the Y_1 error interval is $Y_1 = [4.397, 4.436)$ eV.

The error interval for the work function, C, is the intersection of the Z_1 and Y_1 intervals: $C \in [4.428, 4.436)$ eV. The calculated work function is determined to be 4.432 eV, with an

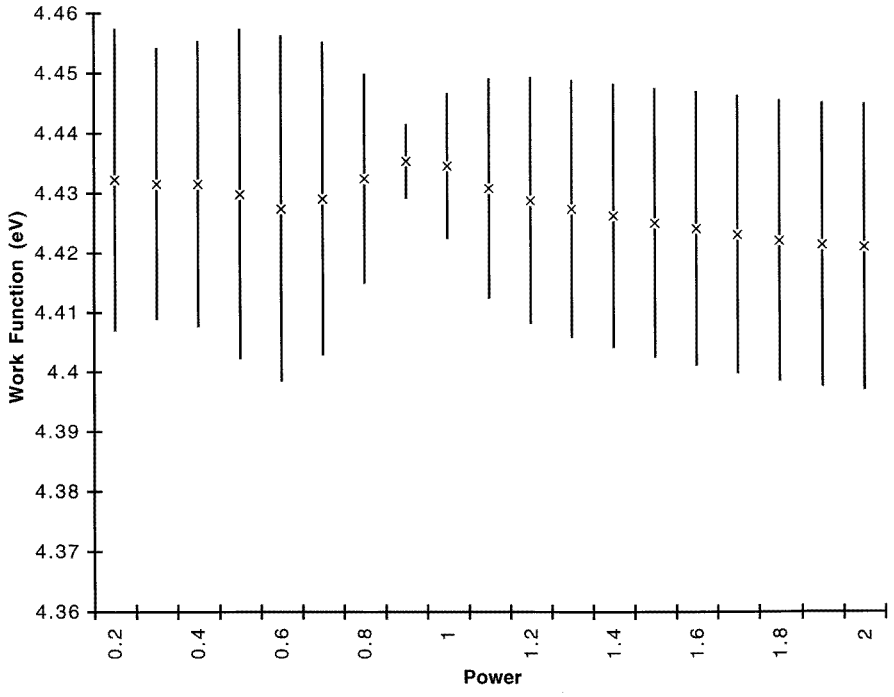

Figure 2. The dependence of the rms difference (error bars) and asymptotic value of the fitting function (crosses) on the power of x.

error interval of only 0.1%. The corresponding experimental error interval is [4.38, 4.44] eV [4]. Thus, the theoretical interval is well within the experimental interval.

Two important phenomena can be observed in figure 2. First, a deviation from the optimal power, $\tilde{\lambda} = 0.9$, results in an increase in the rms difference. The error interval increases, although the limiting value of C is retained. The same phenomenon was observed in the calculated surface relaxation of Al(001) and the work function of Be(0001). A similar conclusion also applies to the surface relaxation of Be(0001) when the intersection with Z_1 is considered.

Second, the asymptotic value corresponding to the optimal power, $A_1[\tilde{\alpha}_1(\tilde{\lambda}), \tilde{\lambda}]$, is stationary with respect to variations in the power. This phenomenon was also observed in the work function and surface relaxation calculations of Al(001) and Be(0001).

3.1.2. Surface relaxation. Since experiment predicts almost no relaxation for the Al(001) surface, the subsurface layers were assumed to be fixed with the bulk inter-layer spacing. Only the spacing between the outermost and second layer was allowed to vary. The surface force acting on the outermost layer was calculated for two different spacings. The surface relaxation was determined by assuming a linear dependence of the force on the spacing.

Surface relaxations were determined for seven special $\boldsymbol{k}$-point sets, consisting of 6, 10, 15, 21, 28, 36, and 45 $\boldsymbol{k}$-points. Figure 3 shows the dependence of the surface relaxation on x. (The surface relaxation was calculated as the ratio of the deviation from the unrelaxed position to the bulk inter-layer separation.)

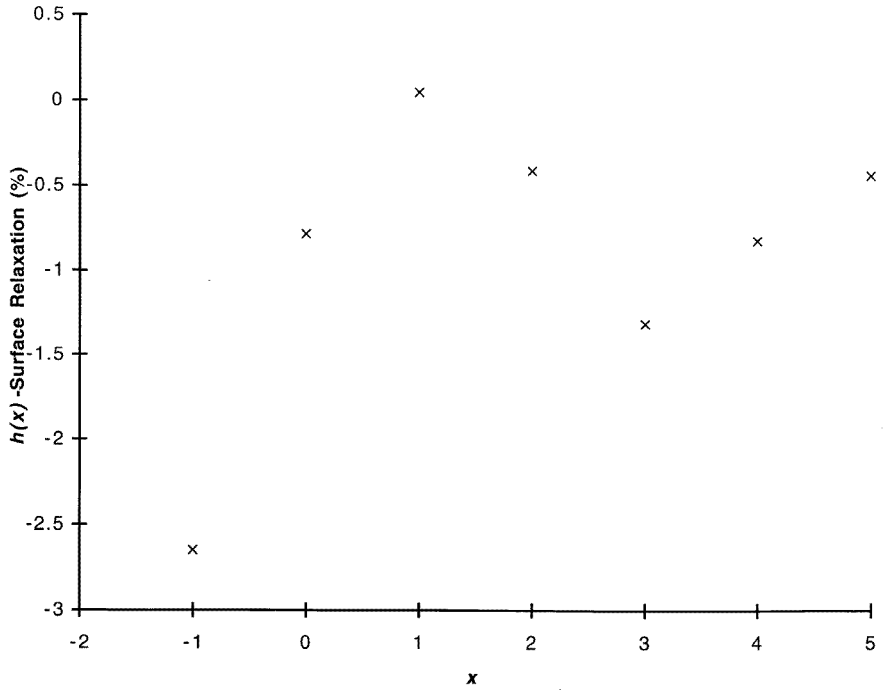

Figure 3. The dependence of the Al(001) surface relaxation on x.

The interval X_1 was taken to be $X_1 = [0, 4]$. The optimal power was 0.9—identical to that obtained for the work function. The Z_1 and Y_1 intervals were calculated to be $Z_1 = [-0.86, -0.54]\%$ and $Y_1 = [-1.42, -0.69)\%$. The uncertainty interval for the surface relaxation, C, the intersection of these two intervals, is given by $C \in [-0.86, -0.69)\%$. This is fairly close to the experimental result of 0% (no experimental error interval has been cited) [5].

3.2. Be(0001)

The calculations were performed using Cunningham's special $\boldsymbol{k}$-points for a hexagonal lattice [6]. Five values of the work function and surface relaxation were obtained, corresponding to 3-, 6-, 18-, 36-, and 108-special $\boldsymbol{k}$-point sets. The variable x was defined such that consecutive special $\boldsymbol{k}$-point sets were spaced by unity. The lower bound of the interval X_1 was set to zero.

3.2.1. Work function. Figure 4 illustrates the oscillatory behaviour of the calculated work function. The interval X_1 was taken to be $X_1 = [0, 4]$. The optimal power was found to be 1.0. The Z_1 and Y_1 intervals were found to be $[5.21, 5.33]$ eV and $[4.58, 5.29)$ eV, respectively. The work function uncertainty interval, $[5.21, 5.29)$ eV, is the intersection of these two intervals. The calculated interval is somewhat outside the experimental interval of $[5.08, 5.12]$ eV [7].

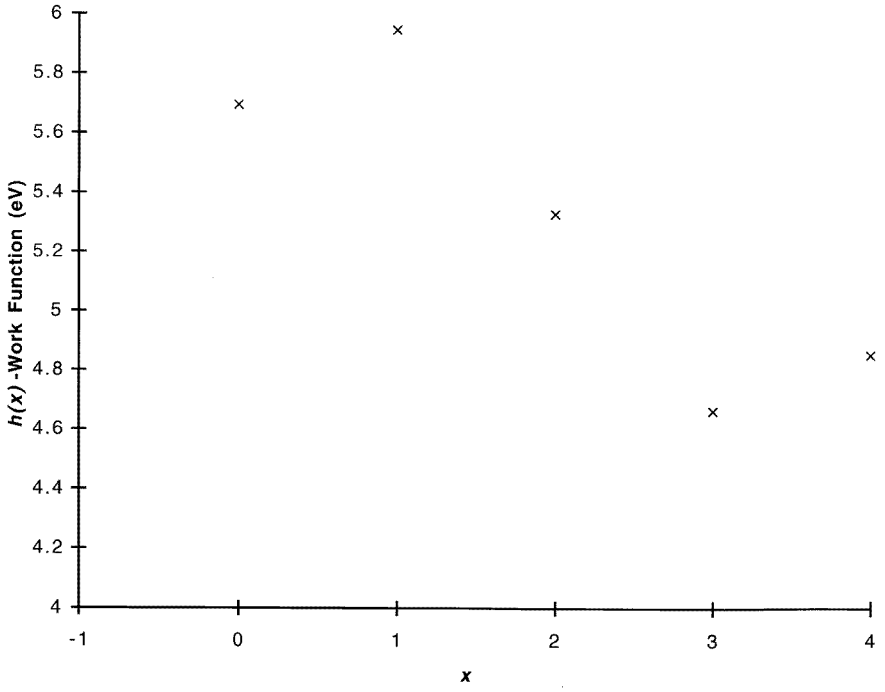

Figure 4. The dependence of the Be(0001) work function on x.

3.2.2. Surface relaxation. Because experiment predicts almost no relaxation of the subsurface layers, the surface relaxation for the top layer was calculated by keeping the lower layers fixed at the bulk inter-layer spacing. The force acting on the top layer was calculated for two different positions of the surface for each set of special $\boldsymbol{k}$-points. The surface relaxation was then determined by assuming a linear dependence of the force on inter-layer spacing. From figure 5 it is apparent that the surface relaxation behaves in an oscillatory manner. The optimal value of the power was found to be 1.0—the same value as for the work function. The Z_1 and Y_1 intervals were found to be $[-0.5, 6.3]$% and $[-3.2, 3.9)$%, respectively. Thus, the calculated uncertainty interval is $[-0.5, 3.9)$%. Again, the calculated result is somewhat outside the experimental interval of $[5.4, 6.2]$% [8]. This appreciable expansion of Be(0001) is considered to be anomalous, since most close-packed surfaces show little, if any, expansion.

4. Conclusion

A general method of evaluating the infinite-$\boldsymbol{k}$ representation of various calculated quantities has been presented. Applications of the method to two test surfaces have been successful, in that agreement with experiment has been good to excellent. The error intervals obtained were generally narrow. Although these calculations were performed with the SEGF method, the technique can be applied to other methods which employ special $\boldsymbol{k}$-point sets.

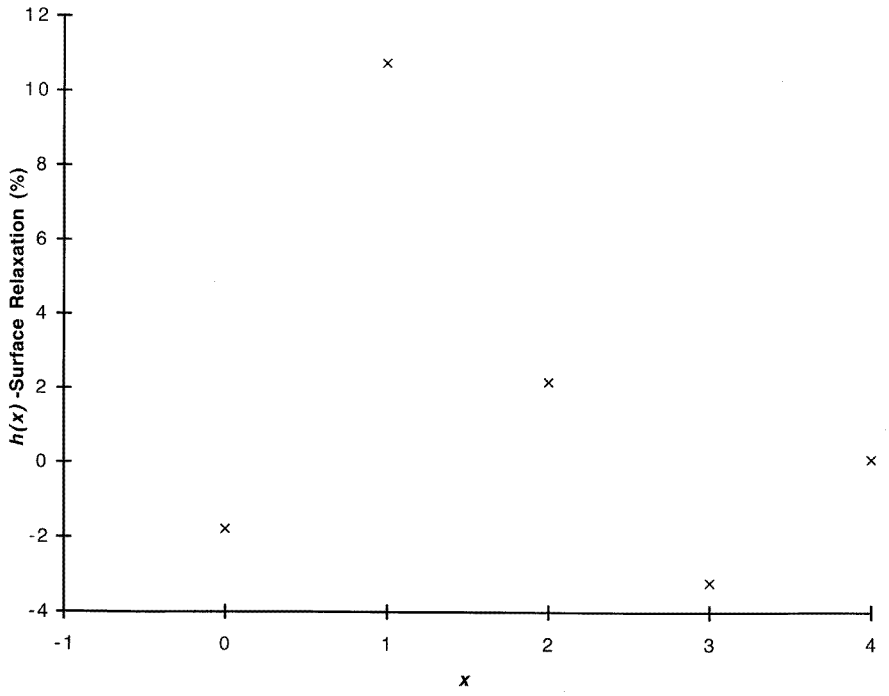

Figure 5. The dependence of the Be(0001) surface relaxation on x.

Appendix

Let $h(x)$ be an arbitrary damped oscillatory function such that for $j = 1, 2, 3, \ldots$

$$\lim_{x\to\infty} h(x) = C \tag{A1}$$

$$[C - h(x_j)][C - h(x_{j+1})] < 0 \tag{A2}$$

and

$$|C - h(x_j)| > |C - h(x_{j+1})| \tag{A3}$$

where x_j and x_{j+1} satisfy the conditions

$$\left.\frac{\mathrm{d}h(x)}{\mathrm{d}x}\right|_{x=x_j} = 0 \tag{A4}$$

$$\left.\frac{\mathrm{d}h(x)}{\mathrm{d}x}\right|_{x=x_{j+1}} = 0 \tag{A5}$$

and

$$\left.\frac{\mathrm{d}h(x)}{\mathrm{d}x}\right|_{x\in(x_j,x_{j+1})} \neq 0. \tag{A6}$$

That is, x_j and x_{j+1} are consecutive turning points, and C is the limiting value of $h(x)$. Let the values of $h(x)$ be known only for the values of x such that

$$x \in X_j = [x_j - \varepsilon_\ell, x_{j+1} + \varepsilon_r] \tag{A7}$$

where ε_ℓ and ε_r are small compared to $x_j - x_{j+1}$.

Inequalities (A2) and (A3) constrain C to be in one of two intervals:

$$C \in Y_j = \left[h(x_{j+1}), \frac{h(x_j) + h(x_{j+1})}{2} \right) \qquad \text{when } h(x_j) > h(x_{j+1}) \tag{A8}$$

or

$$C \in Y_j = \left(\frac{h(x_j) + h(x_{j+1})}{2}, h(x_{j+1}) \right] \qquad \text{when } h(x_j) < h(x_{j+1}). \tag{A9}$$

Let $g(x)$ be a damped harmonic oscillator ($\alpha > 0$) given by

$$g(x) = A + B\,\mathrm{e}^{-\alpha x}\cos(\omega x + \beta). \tag{A10}$$

The aim is to reduce the error interval by fitting $g(x)$ to $h(x)$ over the known interval. Although the turning points of $g(x)$ are equally spaced, those of $h(x)$ may not be. However, a monotonically increasing function $s(x)$ can be defined such that the function $p(x)$ defined by

$$p[s(x)] = h(x)$$

or

$$p(x) = h[s^{-1}(x)] \tag{A11}$$

does have turning points which are uniformly spaced.

Let $s(x)$ depend on x through the parameters $\{\lambda_i\} \equiv \lambda_1, \lambda_2, \ldots, \lambda_n$, i.e., where the $\{\lambda_i\}$ are chosen to minimize the difference between $g[s(x)]$ and $p[s(x)]$. Parameters are chosen such that $g[s(x)]$ and $h(x)$ match at x_j and x_{j+1}, and $\mathrm{d}g[s(x)]/\mathrm{d}x$ vanishes at x_j and x_{j+1}.

These conditions result in the following expressions for ω_j, β_j, B_j and A_j:

$$\omega_j(\{\lambda_i\}) = \frac{\pi}{s(x_{j+1}, \{\lambda_i\}) - s(x_j, \{\lambda_i\})} \tag{A12}$$

$$\beta_j(\alpha_j, \{\lambda_i\}) = -\omega_j(\{\lambda_i\})s(x_j, \{\lambda_i\}) + \tan^{-1}\left(\frac{-\alpha_j}{\omega_j(\{\lambda_i\})}\right) + (j-1)\pi \tag{A13}$$

$$B_j(\alpha_j, \{\lambda_i\}) = \frac{h(x_j) - h(x_{j+1})}{\cos\left[\tan^{-1}(-\alpha_j/\omega_j(\{\lambda_i\})) + (j-1)\pi\right]\{\mathrm{e}^{-\alpha_j s(x_j,\{\lambda_i\})} + \mathrm{e}^{-\alpha_j s(x_{j+1},\{\lambda_i\})}\}} \tag{A14}$$

and

$$A_j(\alpha_j, \{\lambda_i\}) = h(x_j) - \frac{h(x_j) - h(x_{j+1})}{1 + \mathrm{e}^{-\alpha_j \pi/\omega_j(\{\lambda_i\})}}. \tag{A15}$$

From (A15) it can be seen that $A_j(\alpha_j, \{\lambda_i\}) \in Y_j$ for all $\alpha_j \in (0, \infty]$ for a given set $\{\lambda_i\}$. Thus, there exists an $\tilde{\alpha}_j \in (0, \infty]$ such that $A_j(\tilde{\alpha}_j, \{\lambda\}) = C$. This $\tilde{\alpha}_j$ can be approximated as the α_j which minimizes the difference between $p[s(x, \{\lambda_i\})]$ and $g_j[s(x, \{\lambda_i\})]$ in the interval $S_j = [s_j, s_{j+1}]$, where $s_j = s(x_j - \varepsilon_\ell, \{\lambda_i\})$ and $s_{j+1} = s(x_{j+1} + \varepsilon_r, \{\lambda_i\})$. The rms difference between the two functions can be used as a measure of the error. Thus $\tilde{\alpha}_j$ is chosen such that

$$\left.\frac{\mathrm{d}r_j(\alpha_j, \{\lambda_i\})}{\mathrm{d}\alpha_j}\right|_{\alpha_j = \tilde{\alpha}_j} = 0 \tag{A16}$$

where

$$r_j(\alpha_j, \{\lambda_i\}) = \int_{s_j}^{s_{j+1}} \{p[(x, \{\lambda_i\})] - g_j[s(x, \{\lambda_i\}), \alpha_j, \{\lambda_i\}]\}^2\,\mathrm{d}s(x, \{\lambda_i\}). \tag{A17}$$

Condition (A16) results in the following transcendental equation for $\tilde{\alpha}_j$:

$$\int_{s_j}^{s_{j+1}} \mathrm{d}s(x,\{\lambda_i\})\,\{p[s(x,\{\lambda_i\})]-g_j[s(x,\lambda_i),\tilde{\alpha}_j,\{\lambda_i\}]\} \times\frac{\mathrm{d}g_j[s(x,\{\lambda_i\}),\gamma_j(\alpha_j,\{\lambda_i\}),\{\lambda_i\}]}{d\gamma_j(\alpha_j,\{\lambda_i\})}\bigg|_{\alpha_j=\tilde{\alpha}_j}=0 \tag{A18}$$

where $\gamma_j=\mathrm{e}^{-\alpha_j\pi/\omega_j(\{\lambda_i\})}$.

The advantage of switching from α_j to γ_j is that, in solving the transcendental equation (A18), it is easier to look for γ_j in the finite range [0,1), than it is for $\tilde{\alpha}_j\in(0,\infty]$. This is possible because $\partial\gamma_j(\alpha_j,\{\lambda_i\})/\partial\alpha_j\neq 0$. If $h(x)$ is known only for a few values of x, then the integrals in (A17) and (A18) must be replaced by summations.

The rms difference, (A17), can be further minimized by choosing $\{\lambda_i\}$ such that $\mathrm{d}r_j/\,\mathrm{d}\lambda_k|_{\lambda_k=\tilde{\lambda}_k}=0$, for $k=1$ to n.

Next, consider the value of I_j defined by

$$I_j=r_j(\tilde{\alpha}_j,\{\tilde{\lambda}_i\})-\int_{s_{j+1}}^{s_{j+1}+\pi/\omega}\{p[s(x,\{\tilde{\lambda}_i\})]-g[s(x,\{\tilde{\lambda}_i\}),\tilde{\alpha}_j]\}^2\,\mathrm{d}s(x,\{\tilde{\lambda}_i\}). \tag{A19}$$

From (A10) one obtains

$$g[s(x,\{\tilde{\lambda}_i\}),\tilde{\alpha}_j]-A_j(\tilde{\gamma}_j)=-\tilde{\gamma}_j\{g[s(x,\{\tilde{\lambda}_i\})-\pi/\omega_j,\tilde{\alpha}_j)]-A_j(\tilde{\gamma}_j)\} \tag{A20}$$

where $\tilde{\gamma}_j=\gamma_j(\tilde{\alpha}_j,\{\tilde{\lambda}_i\})$.

With the $\{\tilde{\lambda}_i\}$ chosen by minimizing the rms difference, and s_k in close conformity with y_k (the turning points of the approximating functions) such that $[\mathrm{d}g_j(x)/\,\mathrm{d}x]|_{x=y_k}=0$, $\delta_C(x)\in(0,1]$ is defined by

$$p[s(x,\{\tilde{\lambda}_i\})]-C=-\delta_C(x)\{p[s(x,\{\tilde{\lambda}_i\})-\pi/\omega_j]-C\}. \tag{A21}$$

Then

$$p[s(x,\{\tilde{\lambda}_i\})]-A_j(\tilde{\gamma}_j)=-\delta_A(x)\{p[s(x,\{\tilde{\lambda}_i\})-\pi/\omega_j]-A_j(\tilde{\gamma}_j)\} \tag{A22}$$

where $\delta_A(x)\cong\delta_C(x)+\Delta\delta_C(x)$. To first order

$$\Delta\delta_C(x)\cong\frac{\partial\delta_C(x,C)}{\partial C}(A_j(\tilde{\gamma}_j)-C)=(1+\delta_C(x))\frac{C-A_j(\tilde{\gamma}_j)}{p[s(x,\{\lambda_i\})-\pi/\omega_j]-C}. \tag{A23}$$

Using (A20) and (A22), (A19) can be transformed into

$$I_j=\int_{s_j}^{s_{j+1}}\{[\tilde{p}(x)-\tilde{g}_j(x)]^2-[\delta_A(x)\tilde{p}(x)-\tilde{\gamma}\tilde{g}_j(x)]^2\}\,\mathrm{d}s(x,\{\tilde{\lambda}_i\}) \tag{A24}$$

where $\tilde{p}(x)=p(x,\{\tilde{\lambda}_i\})-A_j(\tilde{\gamma}_j)$ and $\tilde{g}_j(x)=g_j[s(x,\{\tilde{\lambda}_i\}),\tilde{\alpha}_j]-\tilde{A}_j(\tilde{\gamma}_j)$.

For a given x, the integrand of (A24) is greater than zero if

$$\delta_A(x)\in W_j=\left(\tilde{\gamma}-(1+\tilde{\gamma}_j)\frac{|\tilde{p}(x)-\tilde{g}_j(x)|}{|\tilde{g}_j(x)|},\tilde{\gamma}+(1+\tilde{\gamma}_j)\frac{|\tilde{p}(x)-\tilde{g}_j(x)|}{|\tilde{g}_j(x)|}\right). \tag{A25}$$

For the ideal case where the functions are identical, $\delta(x)=\tilde{\gamma}_j$ as expected.

If $|\tilde{p}(x)-\tilde{g}_j(x)|$ is approximated by the rms difference, and $\tilde{g}_j(x)$ is evaluated at x_j (to obtain the smallest possible interval), then (A25) simplifies to

$$W_j\supseteq\left(\tilde{\gamma}_j-\frac{\tilde{r}_j(1+\tilde{\gamma}_j)^2}{|\tilde{g}_j(x_j)-\tilde{g}_j(x_{j+1})|},\tilde{\gamma}_j+\frac{\tilde{r}_j(1+\tilde{\gamma}_j)^2}{|\tilde{g}_j(x_j)-\tilde{g}_j(x_{j+1})|}\right) \tag{A26}$$

where $\tilde{r}_j=\{r_j(\tilde{\alpha}_j,\{\tilde{\lambda}_i\})/(s_{j+1}-s_j)\}^{1/2}$.

Now, if $\delta_A(x) \in W_j$ for most x, it follows from (A19) that $I_j > 0$. Thus, as x increases the mean square difference per interval decreases. Consequently,

$$\tilde{r}_j > \lim_{L\to\infty} \left\{ \frac{1}{L - s_j} \int_{s_j}^{L} [p(s(x, \{\tilde{\lambda}_i\})) - g_j(s(x, \{\tilde{\lambda}_i\}), \tilde{\alpha}_j)]^2 \, \mathrm{d}s(x, \{\tilde{\lambda}_i\}) \right\}^{1/2} = \tilde{r}_\infty. \tag{A27}$$

A direct expansion of the integrand leads to

$$\tilde{r}_\infty^2 = [A_j(\tilde{\gamma}_j) - C]^2 + 2[C - A_j(\tilde{\gamma}_j)] \lim_{L\to\infty} \frac{1}{L - s_j} \int_{s_j}^{L} [\hat{p}(x) - \tilde{g}_j(x)] \, \mathrm{d}s(x, \{\tilde{\lambda}_i\}) + \lim_{L\to\infty} \frac{1}{L - s_j} \int_{s_j}^{L} [\hat{p}(x) - \tilde{g}_j(x)]^2 \, \mathrm{d}s(x, \{\tilde{\lambda}_i\}) \tag{A28}$$

where $\hat{p}(x) = p[s(x, \{\tilde{\lambda}_i\})] - C$. Since the integrands in the second and third terms approach zero as x approaches infinity, the corresponding integrals behave like constants as L approaches infinity. As a result, the second and third terms of (A28) vanish. Therefore, it follows that

$$C = A_j(\tilde{\gamma}_j) \pm \tilde{r}_\infty. \tag{A29}$$

Equation (A15) implies that

$$\Delta A_j(\delta_A) \cong \frac{\tilde{g}_j(x_j) - g_j(x_{j+1})}{(1 + \tilde{\gamma}_j)^2} (\delta_A - \tilde{\gamma}_j). \tag{A30}$$

Then, with $|\Delta A_j(\delta)| \cong \tilde{r}_j$,

$$A_j(\delta_A) \in Z_j = (A_j(\tilde{\gamma}_j) - \tilde{r}_j, A_j(\tilde{\gamma}_j) + \tilde{r}_j) \Rightarrow$$
$$\delta_A \in V_j = \left(\tilde{\gamma}_j - \frac{\tilde{r}_j(1 + \tilde{\gamma}_j)^2}{|g_j(x_j) - g_j(x_{j+1})|}, \tilde{\gamma}_j + \frac{\tilde{r}_j(1 + \tilde{\gamma}_j)^2}{|g_j(x_j) - g_j(x_{j+1})|} \right). \tag{A31}$$

Since $V_j \subseteq W_j$, δ_A falls within the interval W_j. Therefore, (A27) and (A29) are appropriate for our damped harmonic oscillator, and they ensure the existence of C in Z_j, the rms error interval of $A_j(\tilde{\gamma}_j)$.

If $Z_j \not\subset Y_j$, the error interval can be reduced further because

$$C \in Y_j \cap Z_j. \tag{A32}$$

If $h(x)$ is known over an interval containing more than two turning points (say N), the error interval can be reduced, since

$$C \in \bigcap_{m=j}^{j+N-2} \{Y_m \cap Z_m\}. \tag{A33}$$

Since many calculated physical quantities behave like $h(x)$ as a function of the number of special $\boldsymbol{k}$-points, intervals (A32) and (A33) are valid error intervals for the infinite-$\boldsymbol{k}$ representation of the system.

References

[1] Benesh G A and Inglesfield J E 1984 *J. Phys. C: Solid State Phys.* **17** 1595
[2] Inglesfield J E and Benesh G A 1988 *Phys. Rev.* B **37** 6682
[3] Monkhorst H J and Pack J D 1976 *Phys. Rev.* B **13** 5188
[4] Grepstad J K, Gartland P O and Slagsvold B J 1976 *Surf. Sci.* **57** 348
[5] Jepsen D W, Marcus P M and Jona F 1972 *Phys. Rev.* B **6** 3684
[6] Cunningham S L 1974 *Phys. Rev.* B **10** 4988
[7] Green A K and Bauer E 1978 *Surf. Sci.* **74** 676
[8] Davis H L, Hannon J B, Ray K B and Plummer E W 1992 *Phys. Rev. Lett.* **68** 2632